

SciEn Conference Series: Engineering Vol. 3, 2025, pp 719-724

https://doi.org/10.38032/scse.2025.3.182

Impact of Particle Size Distribution on Fly Ash-Based Geopolymer Composites

Jasim Ahmed Chowdhury, Md. Shahidul Islam, and Md. Ashraful Islam

Department of Mechanical Engineering, Khulna University of Engineering & Technology, Khulna -9203, Bangladesh

ABSTRACT

This study investigates the properties of fly ash-based composites using particles of varying sizes, sourced from the hopper located immediately before the electrostatic precipitator (ESP) and the final field hopper of the ESP. The research focuses on the development of geopolymer mortars, using sodium silicate and sodium hydroxide as alkali activators (AA). After curing and drying, the samples were analyzed for compressive strength, flexural strength and porosity to assess their physical characteristics. All tests were conducted to evaluate the mechanical performance of different fly ash and activator compositions. The microstructure of the geopolymer samples was examined using scanning electron microscopy, providing insights into the morphological changes associated with the activation process. This investigation highlights the potential of fly ash as a sustainable material for advanced geopolymer applications.

Keywords: Fly ash, ESP, Particle Size, Geopolymer Composite



Copyright @ All authors

This work is licensed under a <u>Creative Commons Attribution 4.0 International License</u>.

1. Introduction

Coal-based power plants produce significant byproducts like bottom ash and fly ash (FA). Bottom ash, settling at the furnace base due to its coarse nature, contrasts with fine fly ash particles captured at various stages, particularly in the Electrostatic Precipitator (ESP). The ESP, utilizing high voltage fields, captures FA efficiently, ensuring environmental compliance by reducing particulate emissions [1].

This study classifies FA into Primary Fly Ash (PFA), collected before the ESP with particle sizes above 10 μm , and Secondary Fly Ash (SFA), collected from the last ESP field, containing finer particles below 10 μm [2]. Two types of FA, pre-ESP (economizer hopper) and post-ESP (last ESP field), were analyzed to evaluate their physical and chemical properties for composite applications.

Geopolymer composites, derived from aluminosilicates and industrial by-products like FA, present eco-friendly alternatives to traditional cement, utilizing waste materials and lowering carbon emissions [3-5]. In Bangladesh, coal plants generate vast amounts of bottom ash and FA, increasing their industrial use [6].

Research highlights include Abdullah et al. [3] on compressive strength in FA-based geopolymer pastes, Morsy et al. [4] on geopolymerization, and Rattanasak et al. [7] on mixing techniques. Nis [8] promoted alkali-activated concrete for waste utilization, while Saloma et al. [5] investigated FA ratios in mortars. Sutcu et al. [9] explored FA and bottom ash in sustainable brick making, finding comparable strength to clay bricks. Wu and Sun et al. [10] emphasized fiber-reinforced geopolymers in high-performance industries [11-13].

Unlike most studies treating FA as uniform, this research examines particle size variation effects on FA composites, advancing material science and optimizing FA utility in engineering applications.

2. Experimental Program

2.1 Materials

In a typical coal-based thermal power plant, initially, coal is transported from the coal stockyard to the coal bunker and then to the coal mill, where it is ground into fine powder before being fed into the furnace for coal combustion. During the coal combustion process, various minerals and impurities present in the coal are released into the boiler furnace as ash particles. Fig.1 Highlights the process of ash production from coal. Fly ashes had been collected from Bangladesh-India Friendship Power Company Limited (BIFPCL).

2.1.1 Primary Fly Ash (PFA)

Fly ash is composed primarily of silicon, aluminum, iron, and calcium oxides. It's known for its pozzolanic properties, which means it can react with lime in the presence of water to form compounds possessing cementitious properties [14]. PFA is derived from the second pass of the furnace, where the economizer circuit is located. This circuit plays a critical role in enhancing the overall efficiency of the power plant by facilitating heat exchange as flue gases pass through. The ash collected here consists of residual materials remaining after coal combustion and heat extraction for power generation. Notably, the collection of this type of ash does not require any external assistance, as it naturally settles within the system. PFA often contains a variety of foreign particles, including unburned carbon, trace metals, and occasionally boiler slag. Scanning Electron Microscope (SEM) analysis at (Fig.2) 170x magnification reveals a diverse range of particle shapes and sizes which indicates that there are others particles except FA, indicative of the complex composition of this ash. Fig. 3 revels the component size of PFA above 10 µm at 4000x zoom.

Energy Dispersive X-ray Spectroscopy (EDS) analysis was conducted to determine the chemical composition of the PFA, which is crucial for predicting the performance and behavior of the resulting geopolymer composites. The chemical composition used in this research work is shown Table 1, providing detailed.

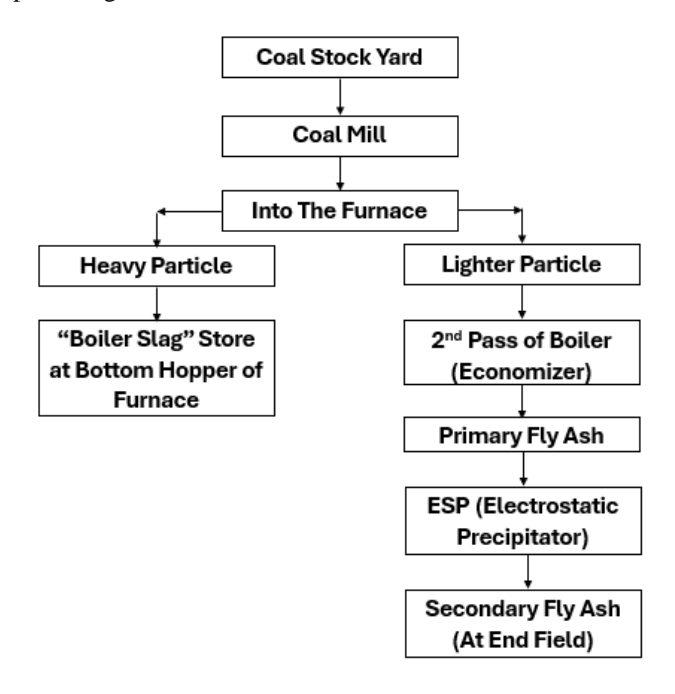


Fig.1 Process of Fly Ash Production from Coal

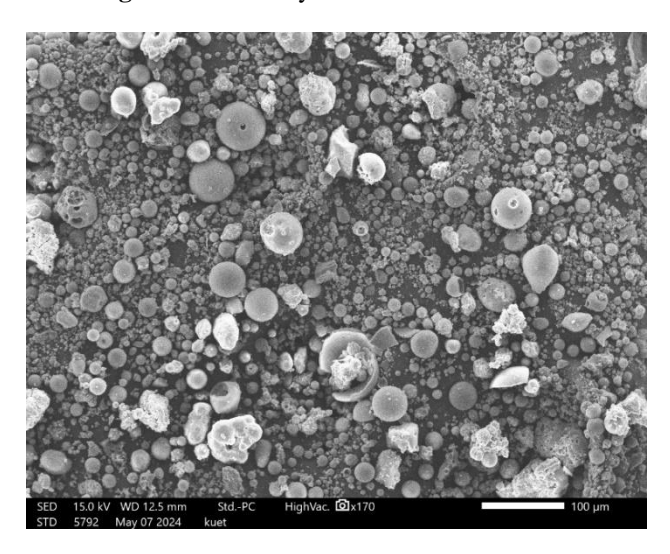


Fig.2 PFA SEM Analysis at 170x Zoom

2.1.2 Secondary Fly Ash (SFA)

The chemical composition of SFA closely resembles that of PFA. However, as indicated by the EDS report (Table 1), the key difference lies in its collection source: the final field of the Electrostatic Precipitator (ESP). This ash undergoes a high-voltage flue gas ionization process, resulting in significantly fewer foreign materials. The SEM image on Fig.4 further corroborates its higher purity, showcasing a more refined particle structure compared to PFA Fig.3. Also, Fig.5 shows the particle size distribution of SFA below $10~\mu m$ at 4000x zoom.

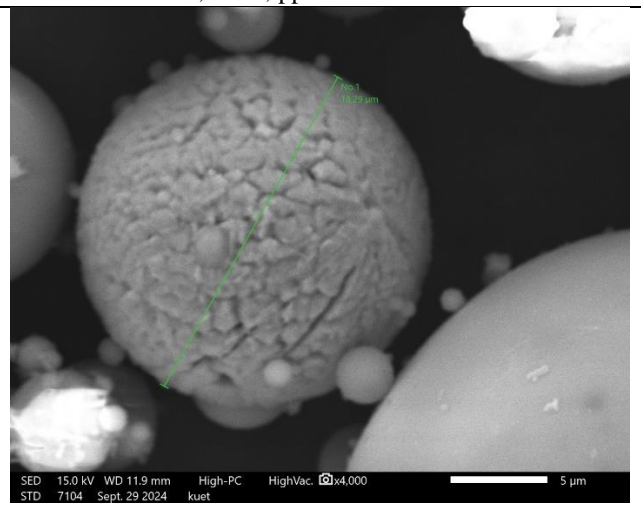


Fig.3 PFA SEM Analysis at 4000x Zoom

Table 1 Composition of Fly Ashes

F A	Ele me nt	Na ₂	Mg O	Al ₂ O	SiO ₂	CaO	FeO
S F A	Mass %	2.63 ±0.5 7	1.58 ±0.4 2	18.9 6±1. 42	47.5 2±2. 45	4.63 ±0.7 8	7.95 ±1.6 7
	Mol%	1.82 ±0.3 9	1.68 ±0.4 5	7.99 ±0.6 0	33.9 ±1.7 5	3.55 ±0.6 0	4.75 ±1.0 0
P F A	Mass %	-	2.95 ±0.5 5	23.2 2±1. 53	53.1 1±2. 54	8.45 ±1.0 1	10.7 5±1. 86
	Mol %	-	4.86 ±0.9 0	15.1 4±1. 00	58.7 7±2. 81	10.0 2±1. 20	9.95 ±1.7 2

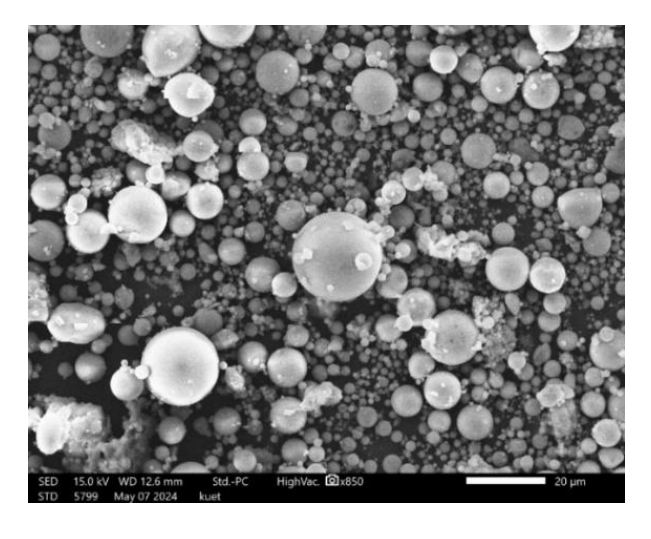


Fig.4 SFA SEM Analysis at 850x Zoom

2.1.3 Sodium Silicate

Sodium silicate, commonly referred to as water glass, is a crucial component in geopolymer synthesis. It creates the ideal alkaline environment and supplies soluble silica, both of which are essential for geopolymer formation and proper hardening. Sodium silicate solutions with 8.23% Na₂O, 29.77% SiO₂ and 62.0% H₂O.

2.5 Sodium Hydroxide

Sodium hydroxide (NaOH) is essential for preparing the alkaline activator solution in geopolymer synthesis. In this research, high-purity NaOH pellets (≥97.0%) from Merck, Germany, were used. A 10M solution was prepared by dissolving 40 g of NaOH in 100 g of distilled water, producing an effective activator after 24 hours.

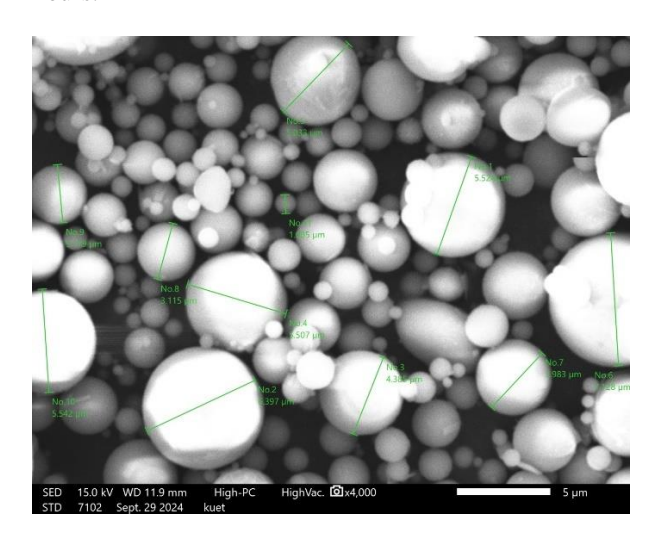


Fig. 5 SFA SEM Analysis at 4000x Zoom

2.2 Composite Preparation

The process begins by preparing and measuring the solid ingredients, such as PFA and SFA. Hereafter mixes the solid ingredients to form a uniform solid state. Further, followed by the preparation and measurement of alkali activators like sodium silicate and sodium hydroxide. The solid ingredients are mixed homogeneously, and the alkali activators are also mixed thoroughly. Both the solid and liquid components are then combined and mixed to form a uniform mixture. This mixture is poured into molds and subjected to oven curing at 70°C for 24 hours. After curing, the material is demolded and subjected to further curing for 7 or 28 days. Finally, the material undergoes testing and characterization to evaluate its properties and performance.

2.3 Material Characterization

Assessing compressive behavior is essential for determining the structural integrity of geopolymer composites. Compression tests were performed on 50x50x50 mm cubic samples prepared according to ASTM-C109. Flexural strength was evaluated following ASTM C78/C78M standards, using 160x40x40 mm samples with a 100 mm span length. Both compressive and flexural tests were conducted using the Shimadzu AGX V 300KN Universal Testing Machine (UTM) following ASTM C109 protocols. The reported compressive strength values represent the average of three tests. All the samples has been cured for 7 days after 24 hours oven curing.

SEM was used in this research to analyze composite materials' surface morphology and to examine fractured surfaces of flexural composites. Samples with heights under 10 mm were dried at 70°C for 24 hours, and samples were imaged for detailed topography and fracture analysis.

Table 2 Composite Indexing of PFA & SFA Geopolymers						
Compo Categ		Alkali-				
site	ory	Activator				
Name	Level	Ratio	Percent	Percent		
		Sodium	age of	age of		
		Silicate/Sod	SFA	PFA		
		ium				
		Hydroxide)				
AE 125	1	1		75		
AE 225	2	1.5	25			
AE 325	3	2	23	73		
AE 425	4	2.5				
AE 150	1	1				
AE 250	2	1.5	50	50		
AE 350	3	2	30	30		
AE 450	4	2.5				
AE 175	1	1				
AE 275	2	1.5	75	25		
AE 375	3	2	15 25			
AE 475	4	2.5				

Table 3 Composite Indexing of Geopolymer Made with FA Collected from Different Stage of ESP

Comp osite Name	Categ ory Level	Alkali- Activator Ratio Sodium Silicate/S odium Hydroxid e)	Percen tage of FA Before Enteri ng ESP	Percen tage of FA at Mid Field ESP	Percen tage of FA Collec ted from End Field ESP	
A 1	1	1				
A 2	2	1.5	100	0	0	
A 3	3	2	100			
A 4	4	2.5				
B 1	1	1				
B 2	2	1.5	0	100	0	
В 3	3	2	U	100	U	
B 4	4	2.5				
C 1	1	1				
C 2	2	1.5				
C 3	3	2	0	0	100	
C 4	4	2.5				

EDS complemented SEM by identifying elements' chemical composition and distribution, particularly in PFA and SFA. For the parametric study on FA, the samples were named and leveled according to Table 2 and Table 3.

3. Results & Discussion

3.1 Compressive Strength Analysis of FA Collected from Different Field of ESP

BIFPCL operates an ESP facility with seven fields. For this study, fly ash was collected from three different stages: before entering the ESP (PFA), at the 4th field (midfield), and from the final field (SFA). The composition for making geopolymers of these samples is detailed in the Table 2.

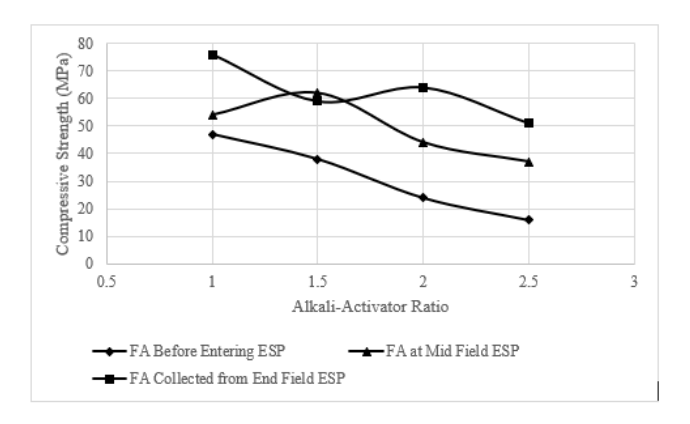


Fig.6 Compressive Strength Vs Alkali-Activator Curve for FA Collected from Different Stage of ESP

The Fig.6 reveals that fly ash (FA) collected before entering the ESP exhibits significantly lower strength compared to the other two stages. In contrast, FA collected at the end of the ESP shows strong performance in terms of strength. However, when the alkali-activator ratio is 1.5, FA from the mid-field demonstrates optimal strength. This suggests that the FA collected at the final ESP field has a more uniform particle distribution, contributing to its superior strength performance.

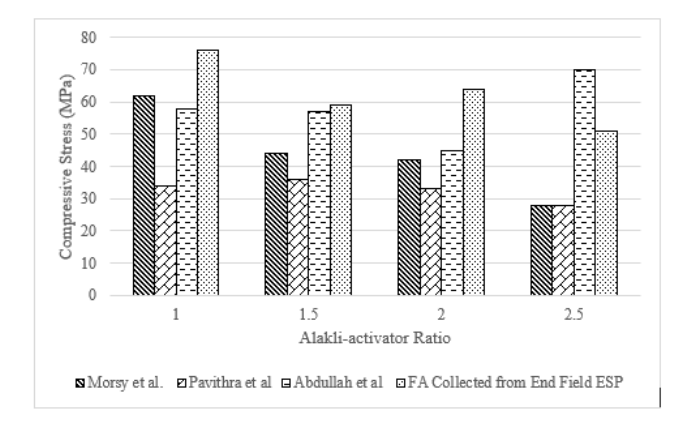


Fig.7 Comparison of Current Study and Previous Study Results of Composites Made with 100% Fly Ash

The Fig. 7 compares the compressive strength of FA collected from the end field of the ESP (labeled as SFA in this study) with three other studies: Morsy et al. [4], Pavithra et al. [15], and Abdullah et al. [3]. It is evident that the SFA from the current study outperforms the results from the

previous studies, except for the study by Abdullah et al., at an alkali-activator ratio of 2.5. However, the highest peak in their study does not surpass the SFA results in the current study.

3.2 Compressive Strength Analysis of Geopolymer Made with PFA & SFA

The Fig.8 shows that as the alkali-activator ratio increases, the trend generally declines, with an exception at a ratio of 2. This anomaly occurs because, at lower alkaliactivator ratios, the increased PFA content caused the paste to solidify during composite mixing. At a ratio of 2, solidification was less pronounced, as it represented a balanced proportion of FA and alkali-activator. However, at a ratio of 2.5, the excess alkali-activator delayed the formation of a hardened composite within the seven-day curing period.

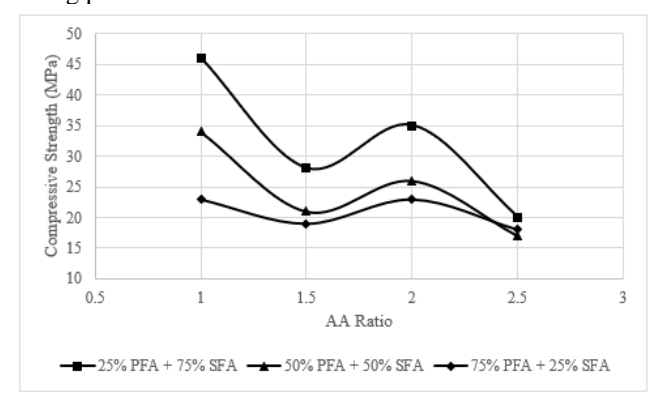


Fig.8 Compressive Strength Vs AA Ratio Curve on Different Variation of PFA & SFA

3.3 Flexural Strength Analysis

The Fig.9 indicates that as the proportion of PFA increases, both the applied force and flexural strength exhibit a downward trend. It was observed that with higher PFA content, the samples tended to bend at the center after oven curing, suggesting significant shrinkage due to rapid heat exposure.

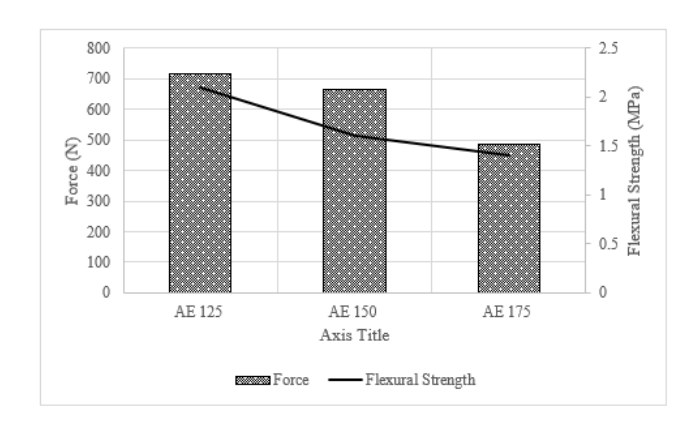


Fig.9 Flexural Strength and Force Curve with variation of PFA

3.4 Compressive Strength after 28 Days of Curing

The Fig.10 shows that after 28 days of curing, AE125 exhibits a significant increase in compressive strength, while the other samples also improve, though to a lesser extent. Notably, AE150 and AE175 show comparatively less improvement between 7 and 28 days.

This is likely because these composites reached maturity during the initial curing period, resulting in minimal further development thereafter.

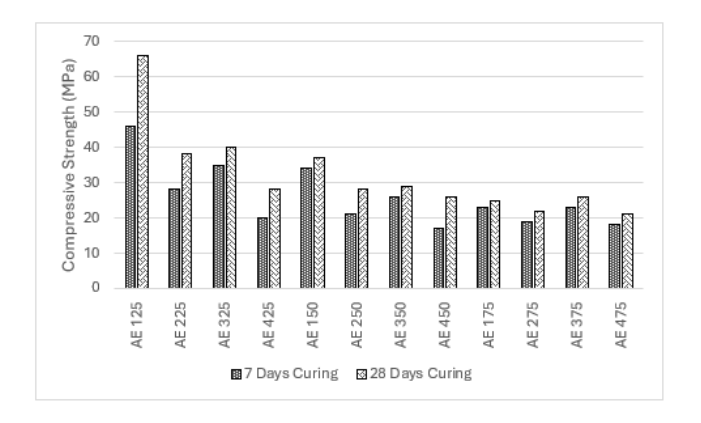


Fig. 10 PFA & SFA Composites Strength After 7 & 28 Days of Curing

3.5 Physical Behavior Analysis

3.5.1 Change of Color and Blow Hole on Surface

As the quantity of PFA ash incorporated into the composite escalated, a conspicuous transformation unfolded, notably altering the visual appearance of the composite's surface. Observations revealed that as the content of PFA increased, a gradual deepening of color occurred, ultimately manifesting as a distinctive black hue. In the illustrative depiction, this alteration was particularly pronounced: at 25% PFA content, the black coloration was discernibly localized, confined to specific regions of the composite's surface Fig.11.



Fig. 11 Change of Color and Blow Hole on Surface of Composites Made with PFA.



Fig.12 Changing color with increasing rate of PFA, lower row left to right for 25% PFA alkali-activator ratio-1,1.5.2,2.5. Upper row left to right for 50% PFA alkaliactivator ratio-1,1.5.2,2.5.

However, as the proportion of PFA surged to 50% and 75%, this darkening effect intensified and diffused more uniformly across the entirety of the surface area. Notably, the sample containing 75% PFA exhibited a more extensive and profound blackening compared to its 50% counterpart, underscoring a progressive relationship between PFA

content and the degree of surface discoloration. This nuanced understanding of the relationship between composition and visual attributes enriches our comprehension of composite behavior and informs strategic decision-making in composite formulation and production processes Fig. 12.

3.5.2 Porosity

During the curing process, water present in the geopolymer mixture can evaporate, leaving behind voids or pores in the material. Rapid evaporation, particularly in hot or dry conditions, can exacerbate porosity formation. With current study also porosity has been measured as per ASTM C373 standard. Table 4 demonstrates that as the proportion of PFA increases, the porosity also rises. This is attributed to PFA's higher water absorption tendency compared to SFA.

Table 4 Physical and mechanical properties of geopolymers

Actual 1	Bulk Density		Porosity			
SFA	PFA	SFA	PFA	25% PFA	50% PFA	75% PFA
1896.24 kg/m ³	2058.74 kg/m ³	1.41	1.54	21.24	23.47 %	32.32 %

3.6 SEM Analysis

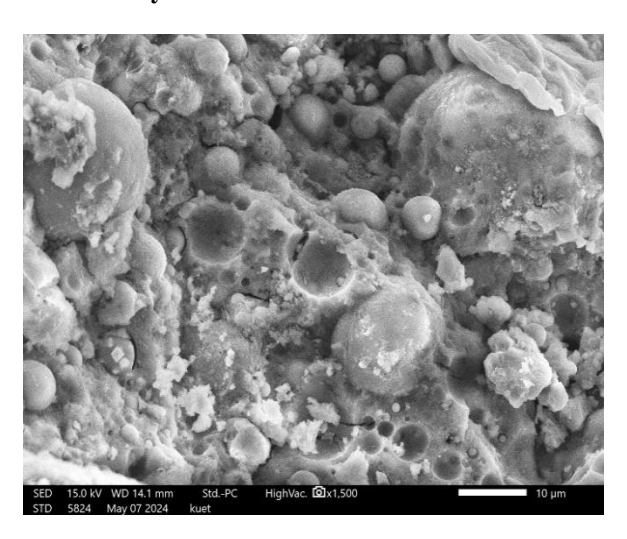


Fig.13 bonding between PFA and SFA, bigger size particles PFA, silicon particles can also be noticed by white jelly form substances

The SEM images in Fig.13 & Fig.14 provide a detailed microstructural analysis of a composite material composed of PFA, SFA, sodium silicate, and sodium hydroxide. In Fig.13, the bonding between particles is highlighted, indicating strong structural integrity and effective curing processes, which are vital for the composite's mechanical strength. The image also reveals particle shapes and sizes, with larger, round particles likely being fly ash cenospheres and smaller, irregular and bigger ones identified as PFA, offering insights into particle integration within the matrix. Surface characteristics, such as roughness and porosity, suggest enhanced bonding potential, while the well-distributed matrix surrounding the particles demonstrates effective interaction between the binder and filler materials. Fig. 14, at higher magnification, provides a closer view of individual particles and microstructural features. Larger spheres represent PFA, while smaller particles are SFA, illustrating their respective contributions to the composite's properties. The image also uncovers porosity and pathways for potential fluid ingress or stress concentration points, along with the degree of particle-matrix interaction, which reflects the quality of composite formation. Additionally, the uniformity of particle distribution and matrix consistency underscores the homogeneity essential for reliable performance.

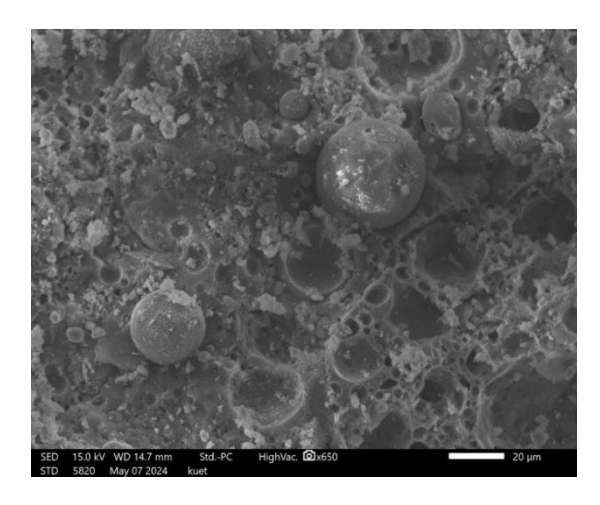


Fig.14 PFA & SFA particles can clearly see

4.0 Conclusion

The current study highlights the characteristics of geopolymer composites prepared with varying particle sizes of fly ash. Key insights include the high-water absorbency of pre-ESP fly ash (PFA), the exceptional compressive strength of 100% final field ESP fly ash (SFA) composites reaching up to 76 MPa due to uniform particle sizes, and the critical role of alkali activator (AA) ratios. The study found that a moderate AA ratio (2:1) optimizes geopolymerization and enhances strength, while excessive activator quantities lead to strength declines due to the presence of unreacted activators. Additionally, increasing the proportion of PFA impacts the composite's surface color. These findings provide valuable insights for future analysis of fly ash-based composites and hold significant potential for advancements in material engineering.

5.0 Acknowledgement

The authors sincerely acknowledge the support of BIFPCL and BHEL, as well as the invaluable laboratory facilities provided by KUET.

References

- [1] R. Świetlik, M. Trojanowska, and M. A. Jóźwiak, "Evaluation of the distribution of heavy metals and their chemical forms in ESP-fractions of fly ash," *Fuel Processing Technology*, vol. 95, pp. 109-118, 2012.
- [2] A. Sarkar, S. Vishwakarma, H. Banichul, K. Mishra, and S. S. Roy, "A comprehensive analysis of the particle size and shape of fly ash from different fields of ESP of a super thermal power plant," *Energy Sources, Part A: Recovery, Utilization, and Environmental Effects*, vol. 34, no. 5, pp. 385-395, 2012.
- [3] M. M. A. Abdullah, H. Kamarudin, M. Bnhussain, I. Khairul Nizar, A. R. Rafiza, and Y. Zarina, "The Relationship of NaOH Molarity, Na₂SiO₃/NaOH Ratio, Fly Ash/Alkaline Activator Ratio, and Curing Temperature to the Strength of Fly Ash-

- Based Geopolymer," *Advanced Materials Research*, vol. 328-330, pp. 1475-1482, 2011.
- [4] M. Morsy, S. Alsayed, Y. Al-Salloum, and T. Almusallam, "Effect of sodium silicate to sodium hydroxide ratios on strength and microstructure of fly ash geopolymer binder," *Arabian journal for science and engineering*, vol. 39, pp. 4333-4339, 2014.
- [5] S. Saloma, H. Hanafiah, D. O. Elysandi, and D. G. Meykan, "Effect of Na2SiO3/NaOH on mechanical properties and microstructure of geopolymer mortar using fly ash and rice husk ash as precursor," in *AIP Conference Proceedings*, 2017, vol. 1903, no. 1: AIP Publishing.
- [6] S. Hossain, A. Dhar, and M. Tamim, "Fly ash in Bangladesh–an overview," *1.27*, vol. 4, p. I011894, 06/01 2013.
- [7] U. Rattanasak and P. Chindaprasirt, "Influence of NaOH solution on the synthesis of fly ash geopolymer," *Minerals Engineering*, vol. 22, no. 12, pp. 1073-1078, 2009.
- [8] A. Niş, "Compressive strength variation of alkali activated fly ash/slag concrete with different NaOH concentrations and sodium silicate to sodium hydroxide ratios," *Journal of Sustainable Construction Materials and Technologies*, vol. 4, no. 2, pp. 351-360, 2019.
- [9] M. Sutcu, E. Erdogmus, O. Gencel, A. Gholampour, E. Atan, and T. Ozbakkaloglu, "Recycling of bottom ash and fly ash wastes in eco-friendly clay brick production," *Journal of Cleaner Production*, vol. 233, pp. 753-764, 2019.
- [10] W. Hwai-Chung and S. Peijiang, "Advanced Construction Materials from Fly Ash," in *Brittle Matrix Composites 7*: Elsevier, 2003, pp. 369-377.
- [11] A. Kinloch, S. Lee, and A. Taylor, "Improving the fracture toughness and the cyclic-fatigue resistance of epoxy-polymer blends," *Polymer*, vol. 55, no. 24, pp. 6325-6334, 2014.
- [12] T. A. Aiken, J. Kwasny, W. Sha, and K. T. Tong, "Mechanical and durability properties of alkaliactivated fly ash concrete with increasing slag content," *Construction and Building Materials*, vol. 301, p. 124330, 2021.
- [13] T. Buasiri, K. Habermehl-Cwirzen, L. Krzeminski, and A. Cwirzen, "Role of carbon nanofiber on the electrical resistivity of mortar under compressive load," *Transportation Research Record*, vol. 2675, no. 9, pp. 32-37, 2021.
- [14] S. Abdullah, L. Ming, M. Abdullah, H. Yong, and K. Zulkifly, "Evaluation on mixing parameter of S/L and Na₂SiO₃/NaOH ratios towards fly ash geopolymers," in *AIP Conference Proceedings*, 2018, vol. 2030, no. 1: AIP Publishing.
- [15] P. Pavithra, M. Srinivasula Reddy, P. Dinakar, B. Hanumantha Rao, B. Satpathy, and A. Mohanty, "Effect of the Na2SiO3/NaOH ratio and NaOH molarity on the synthesis of fly ash-based geopolymer mortar," in *Geo-Chicago 2016*, 2016, pp. 336-344.